Communication System Design and Analysis for Asynchronous Molecular Timing Channels

Nariman Farsad, *Member, IEEE,* Yonathan Murin, *Member, IEEE,* Weisi Guo, *Senior Member, IEEE,* Chan-Byoung Chae, *Senior Member, IEEE,* Andrew Eckford, *Senior Member, IEEE,* and Andrea Goldsmith, *Fellow, IEEE*

***Abstract*—Two new asynchronous modulation techniques for molecular timing (MT) channels are proposed. One based on modulating information on the time between two consecutive releases of *indistinguishable* information particles, and one based on using *distinguishable* particles. For comparison, we consider the synchronized modulation scheme where information is encoded in the time of release and decoded from the time of arrival of particles. We show that all three modulation techniques result in a system that can be modeled as an additive noise channel, and we derive the expression for the probability density function of the noise. Next, we focus on binary communication and derive the associated optimal detection rules for each modulation. Since the noise associated with these modulations has an infinite variance, geometric power is used as a measure for the noise power, and we derive an expression for the geometric SNR (G-SNR) for each modulation scheme. Numerical evaluations indicate that for these systems the bit error rate (BER) is constant at a given G-SNR, similar to the relation between BER and SNR in additive Gaussian noise channels. We also demonstrate that the asynchronous modulation based on two *distinguishable* particles can achieve a BER performance close to the synchronized modulation scheme.**

***Index Terms*—Molecular communication, channel models, noise models, Lévy distribution, stable distributions, bit error rate, and molecular timing channel.**

I. Introduction

MOLECULAR communication is a biologically inspired form of communication, where chemical signals are used to transfer information [3]–[5]. It is possible to modulate information on the particles using different techniques such as concentration [6], type, ratio [7], number [8], time of release [9], or a combination of these techniques [3]. Moreover, information particles can be transported from the transmitter to the receiver using diffusion [10], active transport [11], bacteria [12], and/or flow (or advection) [13]. Between all these techniques, diffusion and flow-based propagation are the easiest to implement, and a few experimental platforms have been built to demonstrate molecular communication based on these transport mechanisms [14]–[16].

In this work we focus on modulation techniques for molecular communication and their corresponding system models. Most prior work on modulation techniques rely on the concentration or the type of the released particles. For example in [17], the order of release of consecutive distinguishable particles is proposed for encoding information. In this work, we consider molecular timing (MT) channels where timing-based modulation is employed. Only a few works have considered this type of modulation: In [9] the time of release of the particles is used for encoding information, while in [18] the information is encoded in the time interval between two pulse releases of information particles.

The work [19] showed that in the case of timing-based modulation, where information is encoded on the release timing of particles, and the transport mechanism is diffusion assisted by constant laminar flow, the channel can be represented as an additive noise channel. In this case the noise term follows the inverse Gaussian (IG) distribution. Capacity bounds for the additive IG noise channel, in bits per channel use, under an average delay constraint, were derived in [19], [20]. In [1], we have shown that in the case of timing-based modulation, where information is encoded on the release timing of particles, and pure diffusive transport (i.e., diffusion without any flow) is employed, the channel can be represented as an additive noise channel where the noise follows the Lévy distribution. The capacity of this channel was studied in [21]–[24], and it was shown that this capacity can increase poly-logarithmically with respect to the number of simultaneously released particles. A sequence detector for this modulation scheme was presented in [25].

In this work, we propose two asynchronous timing-based modulation techniques and compare them with the synchronized timing modulation considered in prior work. These systems can be represented by an additive noise channel, and for diffusion-based MT (DBMT) systems the noise falls in the stable distribution family [26]. Specifically, we consider a synchronized MT system, where information is encoded in the release timing of information particles (system A); an asynchronous MT system where information is encoded in the time between two consecutive releases of *indistinguishable* information particles (system B); and another asynchronous MT system where information is encoded in the time between two consecutive releases of *distinguishable* information particles (system C). Fig. 1 depicts all three systems. One of

This work was been presented in part at the 2015 IEEE Global Communications Conference (GLOBCOM'2015) [1], and at the 2016 IEEE Global Communications Conference (GLOBCOM'2016) [2].

N. Farsad, Y. Murin, and A. Goldsmith are with the Department of Electrical Engineering, Stanford University, Stanford, CA, USA, W. Guo is with the School of Engineering, University of Warwick, Coventry, UK. C.-B. Chae is with the School of Integrated Technology, Yonsei University, Korea. A. Eckford is with the Department of Electrical Engineering and Computer Science, York University, Toronto, Canada.

This research was supported in part by the NSF Center for Science of Information (CSoI) under grant CCF-0939370, and the NSERC Postdoctoral Fellowship fund PDF-471342-2015.

the main motivations for proposing these new modulations is the challenge of synchronization. In particular, for some applications involving micro and nano-scale devices, it may be difficult to synchronize the transmitter and the receiver due to their small size and limited power. In this case, the modulation scheme in system A, which has been used in previous works, may be too difficult to implement in practice. The newly presented modulation schemes in systems B and C, however, do not require synchronization between the transmitter and the receiver. These modulations are analogous to differential phase-shift keying (PSK) in that the asynchronous MT modulations do not require an absolute time reference, while the differential PSK does not require an absolute phase reference.

It must be noted that stable distributed noise arises in system models for a number of different applications. Therefore, the results of this paper could also be applicable in those areas. Specifically, in [27], alpha-stable distributed noise was used to model room acoustics. In radio communications, symmetric alpha-stable distributions were used to model impulsive non-Gaussian noise such as those that exists in ultra-wide bandwidth systems [28], [29]. Capacity bounds for a special class of alpha-stable additive noise channels were provided in [30], [31].

There are only three classes of stable distributions with closed-form probability density functions (PDF) in terms of elementary functions: Gaussian, Cauchy, and Lévy. In this work, we derive closed-form expressions for the PDFs of the noise terms in systems B and C in terms of the complex error function and Voigt functions [32], [33], which are used in other fields of science such as physics. Thus we develop new closed-form PDF results for a subclass of stable noise distributions in terms of the Voigt functions, which can be efficiently calculated numerically [34], [35], and can be approximated using elementary functions in some special cases [36].

To compare the performance of the three proposed modulation schemes, we consider a binary communication system and derive the optimal detection rule for each modulation technique. Since the system noise in all three cases is heavy-tailed with infinite variance, the standard definition of signal power, used in electromagnetic communication, is not suitable. Instead, we derive the expressions for the geometric power [37] of a large class of stable distributions, and use it to represent the noise power. Furthermore, instead of using the well known signal-to-noise ratio (SNR) metric, we use the geometric SNR (G-SNR) [37] metric, which is given by the geometric power of the signal divided by the geometric power of the noise with some normalization constants. Based on numerical evaluations we observe that for the modulations considered, the bit error rate (BER) is constant for a given G-SNR regardless of the geometric signal power and the geometric noise power.

Based on the above derivations, we next use numerical evaluations to compare the BER of all three systems. We show that, as expected, system B with indistinguishable particles exhibits the highest BER, while system A achieves the lowest BER. This indicates that time-synchronized transmission over MT channels, i.e. Modulation A, works better than the other two modulations considered. We further show that by adjusting the diffusion coefficients of the information particles in system C, which is an asynchronous transmission, the BER can approach the BER of system A, where full synchronization is assumed. However, this comes at the cost of added system complexity where both the transmitter and receiver must be capable of transmitting and detecting two distinguishable particles.

The rest of this paper is organized as follows. In Section II we present the three timing-based modulation techniques, and derive an additive noise system model for each of them. In Section III we focus on the diffusion-based propagation and derive the PDF for the additive noise term for each system. In Section IV, binary communication is studied, and the optimal detectors are derived. The geometric power of the noise and the G-SNR of each system are derived in Section V. Numerical BER evaluations of the proposed modulation techniques are presented in Section VI, and concluding remarks are provided in Section VII.

Notation: We denote the set of real numbers by $\mathcal{R}$, and the set of positive real numbers by $\mathcal{R}^+$. Other than these sets, we denote sets with calligraphic letters, e.g., $\mathcal{T}$. We denote random variables (RV)s with upper case letters, e.g., X and Y, and their realizations with the corresponding lower case letters, e.g., x and y. We use $f_Y(y)$ to denote the PDF of a continuous RV Y on $\mathcal{R}$, $f_{Y|X}(y|x)$ to denote the conditional PDF of Y given X, and $F_Y(y)$ and $F_{Y|X}(y|x)$ to denote the corresponding cumulative distribution functions (CDF). We use $\varphi_X(x)$ to denote the characteristic function of the RV X and we use the notation $X \overset{d}{=} Y$ to denote the equality in distribution, i.e., X has the same PDF as Y. We use $|\cdot|$ to denote the absolute value, $j \triangleq \sqrt{-1}$ to denote the imaginary number, and $\Re\{z\}$ to denote the real part of the complex number z. Finally, $\operatorname{erfc}(\cdot)$ is used to denote the complementary error function given by $\operatorname{erfc}(x) = \frac{2}{\sqrt{\pi}} \int_x^\infty e^{-u^2} du$.

II. System Models

In this section we present three different timing-based modulation techniques, which results in three different MT system models. Note that there are no unified channel models for all possible modulation schemes in molecular communication, and typically each modulation yields a different channel model. To develop our model, we make the following assumptions about the system:

A1) The transmitter perfectly controls the release time of each information particle, and the receiver perfectly measures the arrival times of the information particles. Furthermore, the transmitter and the receiver are perfectly synchronized in time, when synchronization is required by the modulation scheme.

A2) Any information particle that arrives at the receiver is absorbed and hence is removed from the propagation medium.

A3) All information particles propagate independently of each other, and their trajectories are random according to an independent and identically distributed (i.i.d.) random process. This is a fair assumption for many different propagation schemes in molecular communication such

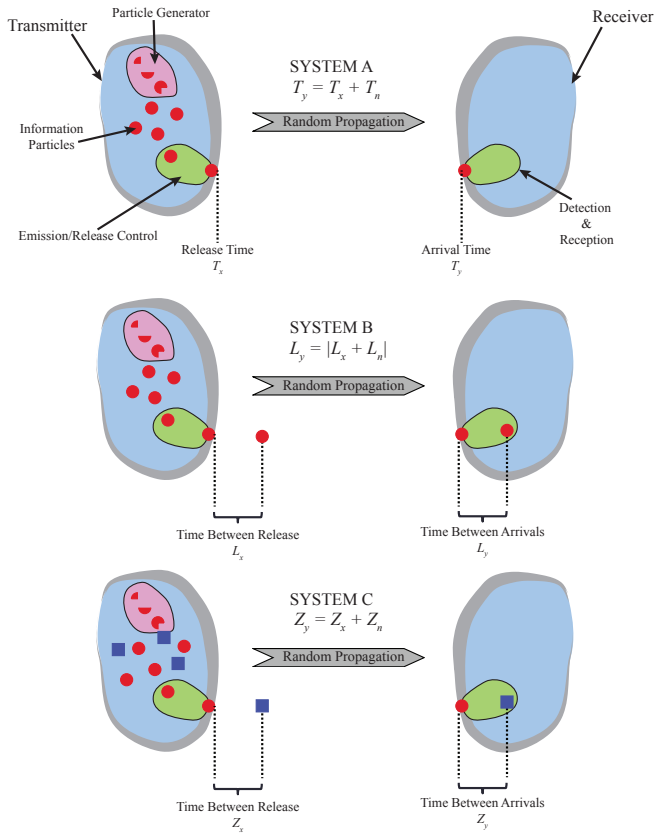

Fig. 1. Summary of the System models corresponding to each modulation scheme. System A: a synchronized MT, system B: an asynchronous MT with indistinguishable information particles, and system C: an asynchronous MT with distinguishable information particles

as diffusion in dilute solutions, i.e., when the number of particles released is much smaller than the number of molecules of the solutions.

A4) There is no inter-symbol interference (ISI) between consecutive channel uses.[1] In practice this assumption can be satisfied if the time between consecutive channel uses is large enough or if chemical reactions are used to dissipate the particles [38].

Note that these assumptions are typical in the study of molecular communication systems.

The first MT system that we consider is the one proposed in [9], [19], where the information is encoded in the release timing of a single information particle. Let $T_x \in \mathcal{T} \subseteq \mathcal{R}^+$ be the release time of the information particle at the transmitter. In this scheme, the information is modulated onto the release time itself. The released particle is then transported from the transmitter to the receiver, where the transport process is random. Let T_y be the time of arrival at the receiver. Then we have

$$T_y = T_x + T_n, \tag{1}$$

where T_n is the random propagation delay of the information particle, which is the *noise term* in this channel. One of the main challenges of this modulation scheme is the need for synchronization between the transmitter and the receiver. In this work, whenever system A is used we assume that the transmitter and the receiver are perfectly synchronized.

To overcome this synchronization challenge, we propose two new modulation schemes in which information is modulated on the time duration *between* two consecutive releases of information particles. The receiver decodes the information from the time between the arrivals of two molecules. Note that in this case synchronization between the transmitter and the receiver is not required. Two cases are possible: either the two released information particles are *indistinguishable* at the receiver, or the two released information particles are *distinguishable* at the receiver.

We first consider the case where both information particles are *indistinguishable*. Without loss of generality, let T_{x_1} be the release timing of the first information particle and let T_{x_2} be the release timing for the second information particle, with $T_{x_2} > T_{x_1}$. Thus, the information is encoded in $L_x = T_{x_2} - T_{x_1}$. Using (1), the system model for this modulation scheme is given by:

$$\begin{aligned} |T_{y_2} - T_{y_1}| &= |T_{x_2} - T_{x_1} + T_{n_2} - T_{n_1}|, \\ L_y &= |L_x + L_n|, \end{aligned} \tag{2}$$

where $L_n = T_{n_2} - T_{n_1}$ is the random noise term in this system, and T_{n_2} and T_{n_1} are the random propagation delays for the first and the second particles as in (1). Note that the absolute value in the system formulation is due to the fact that both information particles are indistinguishable, and therefore the receiver can observe only the absolute difference of arrival times.

The last modulation scheme uses the time between releases of two *distinguishable* information particles (i.e., two different particle types) to encode information. Let T_x^a be the release timing of the type-a information particle and let T_x^b be the release timing of the type-b information particle. We assume that the information is encoded in $Z_x = T_x^b - T_x^a$. Unlike (2) where L_x is always positive, Z_x can be positive or negative depending on the order that the type-a and type-b information particles are released. Using (1), the system model for this scheme is given by:

$$\begin{aligned} T_y^b - T_y^a &= T_x^b - T_x^a + T_n^b - T_n^a, \\ Z_y &= Z_x + Z_n, \end{aligned} \tag{3}$$

where $Z_n = T_n^b - T_n^a$ is the random additive noise term in this system, and T_n^b and T_n^a are the random propagation delays for the type-a and type-b particles as in (1). Again, no synchronization is required between the transmitter and receiver. Fig. 1 summarizes all three modulation techniques.

Note that the proposed modulation schemes and their corresponding system models could be applied to any type of propagation model through the medium as long as Assumptions **A1**)-**A4**) are not violated. In the next section, we derive the distribution of the noise terms for the proposed MT systems, when diffusion propagation is used for particle transport.

[1] In [25] we study communication over DBMT channels in the presence of ISI.

III. Noise Models for DBMT Systems

In the rest of this work we focus on DBMT systems where diffusion is used for particle transport. In particular, in this section we derive the PDF of the noise terms T_n, L_n, and Z_n for DBMT systems in (1)-(3), and discuss some of the properties of these RVs.

A. System A

To specify the random additive noise term T_n in system A, we define a Lévy-distributed RV as follows.

Definition 1 (Lévy Distribution): Let the RV X be Lévy-distributed with location parameter μ and scale parameter c [26]. Then its PDF is given by:

$$f_X(x;\mu,c) = \begin{cases} \sqrt{\frac{c}{2\pi(x-\mu)^3}}\exp\left(-\frac{c}{2(x-\mu)}\right), & x > \mu \\ 0, & x \leq \mu \end{cases}, \quad (4)$$

its characteristic function is given by:

$$\varphi(t;\mu,c) = \exp\left(j\mu t - \sqrt{-2jct}\right), \quad (5)$$

and its CDF is given by:

$$F_X(x;\mu,c) = \begin{cases} \operatorname{erfc}\left(\sqrt{\frac{c}{2(x-\mu)}}\right), & x > \mu \\ 0, & x \leq \mu \end{cases}. \quad (6)$$

Throughout the paper, we use the notation $X \sim \mathscr{L}(\mu,c)$ to indicate a Lévy RV with parameters μ and c.

Assumption **A2**) implies that the distribution of T_n is the distribution of the first hitting time (first arrival at the receiver) of a particle transported via diffusion without flow. In previous works, it was shown that the first hitting time for a diffusion channel with constant drift (i.e., flow) in 1-dimensional space follows the inverse Gaussian distribution [19]. In this work, we consider the pure diffusion channel with no flow. Let d denote the distance between the transmitter and the receiver, and D denote the diffusion coefficient of the information particles in the propagation medium. Following along the lines of the derivations in [19, Sec. II], and using [39, Sec. 2.6.A], it can be shown that for 1-dimensional pure diffusion, the propagation time of each of the information particles follows a Lévy distribution, and therefore the noise in system A is distributed as $T_n \sim \mathscr{L}(0, c_{\mathrm{A}})$ with $c_{\mathrm{A}} = \frac{d^2}{2D}$. Similarly, the conditional PDF $P(T_y|T_x) \sim \mathscr{L}(T_x, c_{\mathrm{A}})$. The PDF and CDF of the standardized (i.e., with $\mu = 0$ and $c_{\mathrm{A}} = 1$) Lévy noise are depicted in Figs. 2 and 3, respectively.

Remark 1: In [40] it is shown that for an infinite, three-dimensional homogeneous medium without flow, and a spherically absorbing receiver, the first arrival time follows a scaled Lévy distribution. Therefore, the results presented in this paper can be extended to 3-D space by simply introducing a scalar multiple in the noise distribution.

B. System B

To find the noise distribution of the system in (2), we first discuss the class of probability distributions known as *stable distributions* [26], [41]. Note that the Lévy distribution belongs to this class.

Definition 2 (Stable Distributions): An RV X has a stable distribution if for two independent copies X_1 and X_2, and positive constants $a_1, a_2, a_3 \in \mathcal{R}^+$ and $a_4 \in \mathcal{R}$, the following holds:

$$a_1 X_1 + a_2 X_2 \overset{d}{=} a_3 X + a_4.$$

Stable distributions can also be defined via their characteristic function.

Definition 3 (Characteristic Function of a Stable Distribution): Let $-\infty < \mu < \infty, c \geq 0, 0 < \alpha \leq 2$, and $-1 \leq \beta \leq 1$. Further define:

$$\Phi(t,\alpha) \triangleq \begin{cases} \tan\left(\frac{\pi\alpha}{2}\right), & \alpha \neq 1 \\ -\frac{2}{\pi}\log(|t|), & \alpha = 1 \end{cases}.$$

Then, the characteristic function of a stable RV X, with location parameter μ, scale parameter c, characteristic exponent α, and skewness parameter β, is given by:

$$\varphi(t;\mu,c,\alpha,\beta) = \exp\left[j\mu t - |ct|^{\alpha}(1 - j\beta\,\mathrm{sgn}(t)\Phi(t,\alpha))\right]. \quad (7)$$

In the following, we use the notation $\mathscr{S}(\mu,c,\alpha,\beta)$ to represent a stable distribution with the parameters μ, c, α, and β. Only the PDFs of three classes of stable distributions are known to have closed-form expressions in terms of elementary functions: the Gaussian distribution with $\alpha = 2$ (the value of β does not matter in this case and can be assumed to be zero), the Lévy distribution with $\alpha = \frac{1}{2}$ and $\beta = 1$, and the Cauchy distribution with $\alpha = 1$ and $\beta = 0$. Generally, the parameters α and β define a subclass within the stable distribution family. Next, we introduce some important properties of stable distributions [26].

Property 1: Let $X \sim \mathscr{S}(\mu,c,\alpha,\beta)$, and define $Y = \frac{X-\mu}{c}$. Then $f(x)dx = f(y)dy$, and Y is called the standard form of X.

Property 2: Let $\tilde{X} \sim \mathscr{S}(0,1,\alpha,\beta)$ be the standard form of a stable RV with parameters α and β. Then the PDF and the CDF of any RV $X \sim \mathscr{S}(\mu,c,\alpha,\beta)$ can be calculated as

$$f_X(x) = \frac{f_{\tilde{X}}\left(\frac{x-\mu}{c}\right)}{c}, \quad (8)$$

$$F_X(x) = F_{\tilde{X}}\left(\frac{x-\mu}{c}\right). \quad (9)$$

Using this property, the standard PDF and CDF of a stable RV can be used to calculate probabilities involving non-standard stable RVs just like the way the standard Gaussian PDF and CDF are used to calculate probabilities involving non-standard Gaussian RVs.

Property 3: The PDFs of stable RVs with $\beta = 0$ are symmetric around μ.

Property 4: If X is a standardized (i.e., with $\mu = 0$ and $c = 1$) stable RV with parameters $0 < \alpha < 2$ and β, then as $x \to \infty$,

$$P(X > x;\alpha,\beta) \approx \frac{1+\beta}{\pi x^{\alpha}}\Gamma(\alpha)\sin\left(\frac{\alpha\pi}{2}\right). \quad (10)$$

Remark 2: Using this property it can be shown that for a stable distributed RV X with parameter α, the moments of

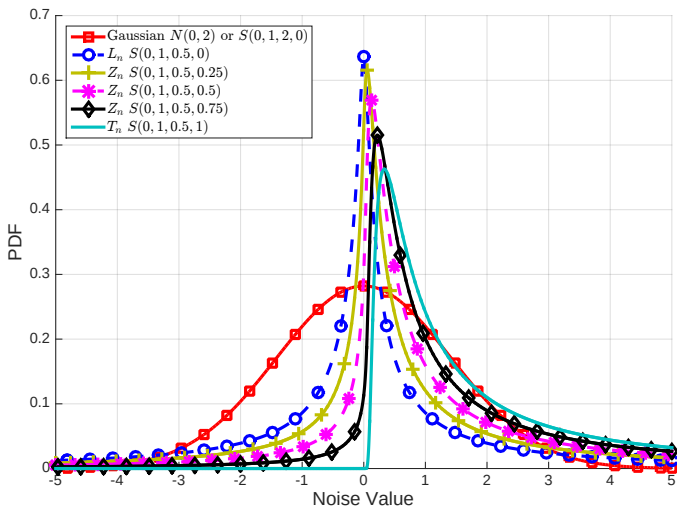

Fig. 2. The probability density function of different standardized noise terms.

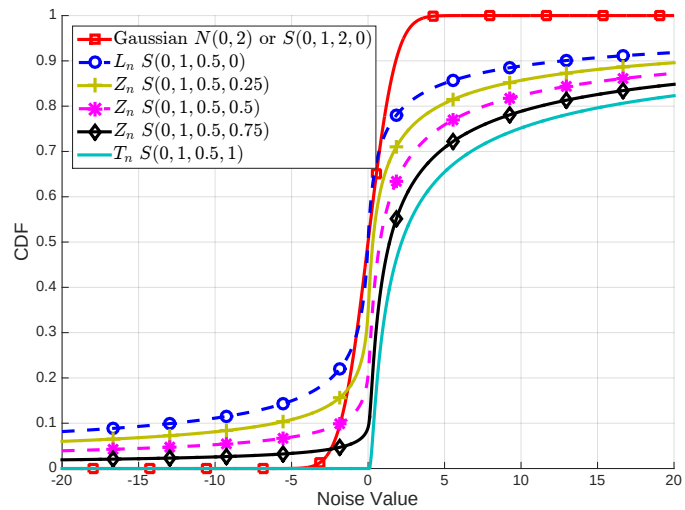

Fig. 3. The cumulative distribution function of different standardized noise terms.

order greater than α (i.e., $\mathbb{E}[|X|^{\alpha}]$) are infinite. Therefore, all stable distributions with $\alpha < 2$ have infinite variances, and all stable distributions with $\alpha < 1$ have infinite mean values.

With these definitions we now model the noise term L_n in (2).

Theorem 1: Let $c_{\mathrm{B}} = \frac{2d^2}{D}$, where d is the distance between the transmitter and the receiver and D is the diffusion coefficient of the information particles. Then, the characteristic function of the noise term L_n is given by:

$$\varphi\left(t; c_{\mathrm{B}}\right) = \exp\left[-\sqrt{c_{\mathrm{B}}|t|}\right],$$

which implies that $L_n \sim \mathscr{S}(0, c_{\mathrm{B}}, \frac{1}{2}, 0)$.

Proof: We know that $L_n = T_{n_2} + (-T_{n_1})$ with $T_{n_2}, T_{n_1} \sim \mathscr{S}(0, c_{\mathrm{A}}, \frac{1}{2}, 1)$, where $c_{\mathrm{A}} = \frac{d^2}{2D}$. Since T_{n_1} and T_{n_2} are independent, the characteristic function for L_n is given by

$$\begin{aligned}\varphi_{L_n}(t) &= \varphi_{T_{n_2}}(t)\varphi_{T_{n_1}}(-t) && (11)\\ &= \exp\left[-\sqrt{|c_{\mathrm{A}}t|}(1 - j\,\mathrm{sgn}(t))\right] \times \\ &\qquad \exp\left[-\sqrt{|c_{\mathrm{A}}t|}(1 + j\,\mathrm{sgn}(t))\right] && (12)\\ &= \exp\left[-\sqrt{|4c_{\mathrm{A}}t|}\right]. && (13)\end{aligned}$$

Thus, using the expression in (7) we conclude that $L_n \sim \mathscr{S}(0, c_{\mathrm{B}}, \frac{1}{2}, 0)$. ■

Remark 3: If the same type of particle is used in system A and system B, and the distance between the transmitter and the receiver is the same, then the scale parameter c in the noise term for system B is four times greater than the scale parameter for system A, i.e., $c_{\mathrm{B}} = 4c_{\mathrm{A}}$.

To find an expression for the PDF of the noise term L_n in (2), we first define the following functions. Let $K(a,b)$ and $L(a,b), a \in \mathcal{R}, b \in \mathcal{R}^+$, be the complex and imaginary Voigt functions [42], given by :

$$K(a,b) \triangleq \frac{1}{\sqrt{\pi}} \int_0^{\infty} \exp(-t^2/4)\exp(-bt)\cos(at)dt, \quad (14)$$

and

$$L(a,b) \triangleq \frac{1}{\sqrt{\pi}} \int_0^{\infty} \exp(-t^2/4)\exp(-bt)\sin(at)dt. \quad (15)$$

The Voigt functions, which are widely used in the fields of physics, astronomy, and chemistry, can be computed efficiently and quickly numerically [34], [35]. Moreover, for some special cases (e.g., $b \gg 0$), analytical approximations of these functions exist in terms of elementary functions [36]. We further define:

$$\begin{aligned}G(u) \triangleq \frac{1}{\sqrt{8\pi|u|^3}} &\left[K\left(-\frac{1}{\sqrt{8|u|}}, \frac{1}{\sqrt{8|u|}}\right)\right.\\ &\left.+L\left(-\frac{1}{\sqrt{8|u|}}, \frac{1}{\sqrt{8|u|}}\right)\right]. \quad (16)\end{aligned}$$

The PDF of L_n is stated in the following theorem:

Theorem 2: Let $L_n \sim \mathscr{S}(0, c_{\mathrm{B}}, \frac{1}{2}, 0)$. Then the PDF of L_n is given by:

$$f_{L_n}(\ell_n) = \begin{cases} \frac{1}{c_{\mathrm{B}}} G\left(\frac{\ell_n}{c_{\mathrm{B}}}\right), & \ell_n \neq 0 \\ \frac{2}{c_{\mathrm{B}}\pi}, & \ell_n = 0 \end{cases}. \quad (17)$$

Proof: The proof is provided in Appendix A. ■

In this work, we do not provide an expression for the CDF of the noise terms $F_{L_n}(\ell_n)$, and it would be difficult to integrate (2) to obtain the CDF. However, the CDF can be calculated numerically using the methods described in [43, Sec. 3]. Moreover, tables of the standardized CDF could be used to calculate probabilities involving the noise term. Figs. 2 and 3 depict the PDF and CDF for the standardized noise term L_n with $c_{\mathrm{B}} = 1$.

C. System C

We first note that the noise Z_n given in (3) is fundamentally different from the noise L_n in system B since the two different types of information particles may have different diffusion coefficients. Let D_a be the diffusion coefficient of information particle a, and D_b be the diffusion coefficient for

the information particle b. We define $c_{\mathrm{C}} \triangleq \frac{d^2(\sqrt{D_a}+\sqrt{D_b})^2}{2D_aD_b}$, $\beta_{\mathrm{C}} \triangleq \frac{\sqrt{D_a}-\sqrt{D_b}}{\sqrt{D_a}+\sqrt{D_b}}$. Furthemore, without loss of generality, we assume that particle a is released before particle b. We now model the noise term Z_n in (3).

Theorem 3: The characteristic function for the noise term Z_n is given by:

$$\varphi\left(t; c_{\mathrm{C}}, \beta_{\mathrm{C}}\right) = \exp\left[-\sqrt{c_{\mathrm{C}}|t|}\left(1 - j\beta_{\mathrm{C}}\,\mathrm{sgn}(t)\right)\right],$$

which implies that $Z_n \sim \mathscr{S}\left(0, c_{\mathrm{C}}, \frac{1}{2}, \beta_{\mathrm{C}}\right)$.

Proof: First, note that $Z_n = T_{n_b} + (-T_{n_a})$ with $T_{n_a}, T_{n_b} \sim \mathscr{S}(0, c_i, \frac{1}{2}, 1)$, where $c_i = \frac{d^2}{2D_i}$ for $i \in \{a, b\}$. Since T_{n_a} and T_{n_b} are independent, the characteristic function of Z_n is given by:

$$\begin{aligned}
\varphi_{Z_n}(t) &= \varphi_{T_{n_b}}(t)\varphi_{T_{n_a}}(-t) && (18)\\
&= \exp\left[-\sqrt{c_b}\sqrt{|t|}(1 - j\,\mathrm{sgn}(t))\right] \times \\
&\qquad \exp\left[-\sqrt{c_a}\sqrt{|t|}(1 + j\,\mathrm{sgn}(t))\right] && (19)\\
&= \exp\left[-\sqrt{|t|}(\sqrt{c_b} + \sqrt{c_a} - j\,\mathrm{sgn}(t)(\sqrt{c_a} - \sqrt{c_b}))\right] && (20)\\
&= \exp\Bigg[-(\sqrt{c_b} + \sqrt{c_a})\sqrt{|t|} \\
&\qquad \left(1 - j\,\mathrm{sgn}(t)\frac{\sqrt{c_a} - \sqrt{c_b}}{\sqrt{c_b} + \sqrt{c_a}}\right)\Bigg] && (21)\\
&= \exp\Bigg[-\frac{d(\sqrt{D_a} + \sqrt{D_b})}{\sqrt{2D_aD_b}}\sqrt{|t|} \\
&\qquad \left(1 - j\frac{\sqrt{D_a} - \sqrt{D_b}}{\sqrt{D_a} + \sqrt{D_b}}\,\mathrm{sgn}(t)\right)\Bigg]. && (22)
\end{aligned}$$

Thus, using the expression in (7) we conclude that $Z_n \sim \mathscr{S}\left(0, c_{\mathrm{C}}, \frac{1}{2}, \beta_{\mathrm{C}}\right)$. ■

Remark 4: When the diffusion coefficients of the two particles are approximately the same, i.e., $D_a \approx D_b$, the distribution of Z_n approaches the distribution L_n (i.e. $\beta_{\mathrm{C}} \approx 0$). On the other hand, when $D_a \ll D_b$ or $D_a \gg D_b$, then $\beta_{\mathrm{C}} \approx \pm 1$ which implies that Z_n is Lévy distributed. Therefore, when one information particle has a much higher diffusion coefficient than the other, system C can be reduced to system A with the added benefit that no synchronization is required between the transmitter and the receiver. However, this comes at a cost of: 1) Using two particles instead of one; and 2) The resulting system A has a scaling parameter that corresponds to the smaller diffusion coefficient.

To derive the PDF of Z_n we first define the following two functions:

$$\begin{aligned}
G_+(u, \beta) &\triangleq \frac{1}{\sqrt{8\pi|u|^3}}\Bigg[(1+\beta)K\left(-\frac{1+\beta}{\sqrt{8|u|}}, \frac{1-\beta}{\sqrt{8|u|}}\right) \\
&\qquad +(1-\beta)L\left(-\frac{1+\beta}{\sqrt{8|u|}}, \frac{1-\beta}{\sqrt{8|u|}}\right)\Bigg], && (23)\\
G_-(u, \beta) &\triangleq \frac{1}{\sqrt{8\pi|u|^3}}\Bigg[(1-\beta)K\left(\frac{1-\beta}{\sqrt{8|u|}}, \frac{1+\beta}{\sqrt{8|u|}}\right) \\
&\qquad +(1+\beta)L\left(\frac{1-\beta}{\sqrt{8|u|}}, \frac{1+\beta}{\sqrt{8|u|}}\right)\Bigg], && (24)
\end{aligned}$$

where $K(a, b)$ and $L(a, b)$ are the real and imaginary Voigt functions given in (14) and (15), respectively. The PDF of Z_n is now stated in the following theorem:

Theorem 4: Let $Z_n \sim \mathscr{S}(0, c_{\mathrm{C}}, \frac{1}{2}, \beta_{\mathrm{C}})$. Then the PDF of Z_n is given by:

$$f_{Z_n}(z_n) = \begin{cases} \frac{1}{c_{\mathrm{C}}}G_+\left(\frac{z_n}{c_{\mathrm{C}}}, \beta_{\mathrm{C}}\right), & z_n > 0 \\ \frac{2(1-\beta^2)}{c_{\mathrm{C}}\pi(1+\beta^2)^2}, & z_n = 0 \\ \frac{1}{c_{\mathrm{C}}}G_-\left(\frac{z_n}{c_{\mathrm{C}}}, \beta_{\mathrm{C}}\right), & z_n < 0 \end{cases}. \qquad (25)$$

Proof: The proof is provided in Appendix B. ■

Again, we do not provide an expression for the CDF of the noise terms $F_{Z_n}(z_n)$, instead we note that it can be numerically calculated using the methods of [43, Sec. 3]. Figs. 2 and 3 depict the PDF and CDF for the standardized noise term Z_n with $c_{\mathrm{C}} = 1$ and four different values for β_{C}. Note that for $\beta_{\mathrm{C}} = 0$ the distribution and the density functions of the noise Z_n in System C are the same as the noise L_n in system B. This is due to the diffusion coefficient of type-a and type-b particles being equal, which means that both particle types have the same random propagation delay characteristics.

IV. Optimal Detection in Binary DBMT Systems

In this section, we consider equiprobable binary transmission over the three different DBMT systems. Using the noise models developed in the previous section, we characterize the optimal detection rule for each modulation.

A. System A

For system A, w assume that the transmission symbols are $T_x \in \{0, \Delta\}$, where $\Delta > 0$. Using Property 2, we write the distribution of the output probability, conditioned on the input, in terms of the standard Lévy distribution $\tilde{T}_n \sim \mathscr{L}(0, 1)$ as follows:

$$f_{T_y|T_x}(t_y|T_x = 0) = f_{T_n}(t_y) = \frac{f_{\tilde{T}_n}(t_y/c_{\mathrm{A}})}{c_{\mathrm{A}}}, \qquad (26)$$

$$f_{T_y|T_x}(t_y|T_x = \Delta) = f_{T_n}(t_y - \Delta) = \frac{f_{\tilde{T}_n}\left((t_y - \Delta)/c_{\mathrm{A}}\right)}{c_{\mathrm{A}}}. \qquad (27)$$

As the two transmitted symbols are equiprobable, the detector that minimizes the probability of error is the maximum likelihood (ML) detector. In this work we assume both the 0-bit and the 1-bit are equiprobable and apply the ML detector. In this case, the likelihood ratio is given by:

$$\Lambda_A(t_y) = \frac{f_{T_y|T_x}(t_y|T_x = 0)}{f_{T_y|T_x}(t_y|T_x = \Delta)}, \qquad (28)$$

and optimal detection can be done by a comparison of the log likelihood ratio (LLR) to zero, i.e.,

$$\log(\Lambda_A(t_y)) \underset{T_x = \Delta}{\overset{T_x = 0}{\gtrless}} 0. \qquad (29)$$

Note that the proof of the existence of the optimal threshold value is straightforward using the fact that stable distributions

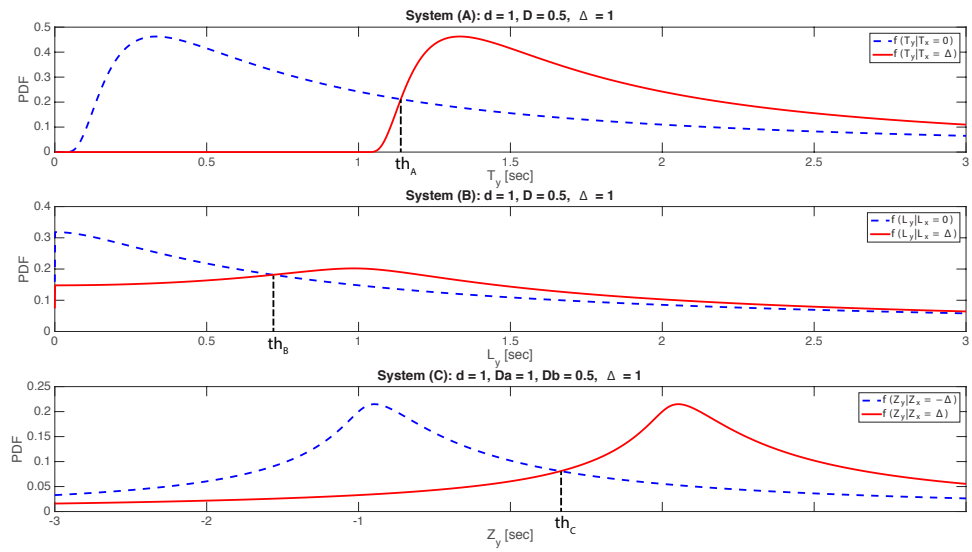

Fig. 4. The ML optimal decision threshold for the three systems.

are unimodal [41, Theorem 2.7.6], and that for the noise term T_n the mode is at $c/3$. Therefore, there exists a threshold $\Delta < \text{th}_\text{A} \leq c/3 + \Delta$, such that $\Lambda_A(t) > 1$ for $t < \text{th}_\text{A}$ and $\Lambda_A(t) \leq 1$ for $t \geq \text{th}_\text{A}$ [44], [45]. The top plot in Figure 4 shows the optimal threshold for the case when $\Delta = 1$, the distance is $d = 1$ and the diffusion coefficient is $D = 0.5$.

The probability of error for system A is now given by:

$$\begin{aligned} P_e^A &= P(T_x = 0)\Pr(t_y > \text{th}_\text{A}|T_x = 0) \\ &\quad + P(T_x = \Delta)\Pr(t_y \leq \text{th}_\text{A}|T_x = \Delta), && (30) \\ &= 0.5\Pr(t_n > \text{th}_\text{A}) + 0.5\Pr(t_n \leq \text{th}_\text{A} - \Delta) && (31) \\ &= 0.5[1 - F_{\tilde{T}_n}(\tfrac{\text{th}_\text{A}}{c_\text{A}}) + F_{\tilde{T}_n}(\tfrac{\text{th}_\text{A}-\Delta}{c_\text{A}})], && (32) \end{aligned}$$

where $F_{\tilde{T}_n}(t)$ is the CDF of a standard Lévy RV.

B. System B

For system B we assume that the input is $L_x \in \{0, \Delta\}$, where $L_x = 0$ represents two particles released simultaneously, while $L_x = \Delta$ represents two particles released Δ seconds apart. Let $\tilde{L}_n \sim \mathscr{S}(0, 1, \frac{1}{2}, 0)$ be the standard form of the noise term in (2). The PDF of the output L_y, given the input L_x, is provided in the following proposition:

Proposition 1: The system output L_y, given the system input L_x, has the PDF:

$$f_{L_y|L_x}(\ell_y|L_x = 0) = \begin{cases} \frac{2 f_{\tilde{L}_n}\left(\frac{\ell_y}{c_\text{B}}\right)}{c_\text{B}} & \ell_y > 0 \\ \frac{2}{(c_\text{B}\pi)} & \ell_y = 0 \\ 0 & \ell_y < 0 \end{cases}, \tag{33}$$

$$f_{L_y|L_x}(\ell_y|L_x = \Delta) = \begin{cases} \frac{f_{\tilde{L}_n}\left(\frac{\ell_y-\Delta}{c_\text{B}}\right)+f_{\tilde{L}_n}\left(\frac{-\ell_y-\Delta}{c_\text{B}}\right)}{c_\text{B}} & \ell_y > 0 \\ \frac{f_{\tilde{L}_n}\left(\frac{\Delta}{c_\text{B}}\right)}{c_\text{B}} & \ell_y = 0 \\ 0 & \ell_y < 0 \end{cases}. \tag{34}$$

Proof: It is clear from the system definition that when $L_y < 0$ the PDF is 0 (i.e. the time between two arrival times is not negative). When $L_y = 0$, we have $f_{L_y|L_x}(0|L_x = 0) = f_{L_n}(0)$, and $f_{L_y|L_x}(0|L_x = \Delta) = f_{L_n}(\Delta)$. To derive the PDF value for $L_y > 0$, we use the fact that the CDF of L_y given $L_x = x \geq 0$ can be obtained from the CDF of $\tilde{L}_n$ as

$$\begin{aligned} F_{L_y|L_x}(\ell_y|L_x = x) &= \Pr(L_y \leq \ell_y|L_x = x) \\ &= \Pr(|x + L_n| \leq \ell_y) \\ &= \Pr(-\ell_y \leq x + L_n \leq \ell_y) \\ &= \Pr(\tfrac{-\ell_y - x}{c_\text{B}} \leq \tilde{L}_n \leq \tfrac{\ell_y - x}{c_\text{B}}) \\ &= F_{\tilde{L}_n}\left(\tfrac{\ell_y - x}{c_\text{B}}\right) - F_{\tilde{L}_n}\left(\tfrac{-\ell_y - x}{c_\text{B}}\right). \end{aligned}$$

By differentiating with respect to ℓ_y, and setting $x = 0$ and $x = \Delta$, we obtain (33) and (34), respectively. ■

Similarly to (28), the likelihood ratio for the ML detector for system B is given by:

$$\Lambda_B(\ell_y) = \frac{f_{L_y|L_x}(\ell_y|L_x = 0)}{f_{L_y|L_x}(\ell_y|L_x = \Delta)}. \tag{35}$$

The following theorem states that, just like in the case of system A, the ML detector can be implemented by comparing $\log(\Lambda_B(\ell_y))$ to zero:

Theorem 5: There exists a fixed threshold $\text{th}_\text{B} > \frac{\Delta}{2}$ such that the ML detector in the case of system B is given by:

$$\log(\Lambda_B(\ell_y)) \underset{T_x = \Delta}{\overset{T_x = 0}{\gtrless}} 0. \tag{36}$$

Proof: The proof is provided in Appendix C. ■

The middle plot in Figure 4 depicts the optimal threshold for the case when $\Delta = 1$, the distance is $d = 1$ and the diffusion coefficient is $D = 0.5$. Since the closed-form expression for the CDF of the noise term is unknown, this threshold is calculated numerically. Finally, the probability of error for

binary communication over system B is given by:

$$\begin{aligned} P_e^B &= P(L_x=0)\Pr(L_y > \mathsf{th}_\mathsf{B}|L_x=0) \\ &\quad + P(L_x=\Delta)\Pr(L_y \le \mathsf{th}_\mathsf{B}|L_x=\Delta), \\ &= 0.5(\Pr(L_n > \mathsf{th}_\mathsf{B}) + \Pr(L_n \le -\mathsf{th}_\mathsf{B})) \\ &\quad + 0.5\Pr(-\mathsf{th}_\mathsf{B}-\Delta \le L_n \le \mathsf{th}_\mathsf{B}-\Delta), \\ &= 0.5(\Pr(\tilde{L}_n > \tfrac{\mathsf{th}_\mathsf{B}}{c_\mathsf{B}}) + \Pr(\tilde{L}_n \le -\tfrac{\mathsf{th}_\mathsf{B}}{c_\mathsf{B}})) \\ &\quad + 0.5\Pr(\tfrac{-\mathsf{th}_\mathsf{B}-\Delta}{c_\mathsf{B}} \le \tilde{L}_n \le \tfrac{\mathsf{th}_\mathsf{B}-\Delta}{c_\mathsf{B}}), \\ &= F_{\tilde{L}_n}\big(\tfrac{\mathsf{th}_\mathsf{B}}{c_\mathsf{B}}\big) + 0.5\big(F_{\tilde{L}_n}\big(\tfrac{\mathsf{th}_\mathsf{B}-\Delta}{c_\mathsf{B}}\big) - F_{\tilde{L}_n}\big(\tfrac{\mathsf{th}_\mathsf{B}+\Delta}{c_\mathsf{B}}\big)\big). \end{aligned} \tag{37}$$

Thus, similarly to the case of system A, the probability of error can be calculated using the standard form of the noise term.

C. System C

Recall that for system C the two particles are *distinguishable*, and $Z_x = T_{x_b} - T_{x_a}$ is the time interval between the releases of particles b and a. Here, we assume information is encoded in the *order* of release. The input $Z_x \in \{-\Delta, \Delta\}$ is now given by:

$$Z_x = \begin{cases} \Delta, & T_{x_a} = 0, T_{x_b} = \Delta \\ -\Delta, & T_{x_b} = 0, T_{x_a} = \Delta \end{cases}. \tag{38}$$

Note that similarly to systems A and B, the information is encoded over the time period Δ.

Let $\tilde{Z}_n \sim (0, 1, \frac{1}{2}, \beta_\mathrm{C})$ be the standard form of the noise term in (3). Then the PDF of the output given the input is given by

$$f_{Z_y|Z_x}(z_y|Z_x=-\Delta) = \frac{f_{\tilde{Z}_n}\big(\frac{z_y+\Delta}{c_\mathrm{C}}\big)}{c_\mathrm{C}} \tag{39}$$

$$f_{Z_y|Z_x}(z_y|Z_x=\Delta) = \frac{f_{\tilde{Z}_n}\big(\frac{z_y-\Delta}{c_\mathrm{C}}\big)}{c_\mathrm{C}}. \tag{40}$$

Again, to minimize the probability of error at the receiver, the ML detector is used. Let th_C be the optimal ML detection threshold for this system. It is easy to see that this threshold exists for system C since stable distributions are unimodal and the two PDFs are shifted versions of each other. The bottom plot in Figure 4 shows the optimal threshold for the case when $\Delta = 1$, the distance is $d = 1$ and the diffusion coefficients are $D_a = 1$ and $D_b = 0.5$. The probability of error is now given by:

$$\begin{aligned} P_e^C &= P(Z_x=-\Delta)\Pr(z_y > \mathsf{th}_\mathsf{C}|Z_x=-\Delta) \\ &\quad + P(Z_x=\Delta)\Pr(z_y \le \mathsf{th}_\mathsf{C}|Z_x=\Delta), \\ &= 0.5\Pr(z_n > \mathsf{th}_\mathsf{C}+\Delta) + 0.5\Pr(z_n \le \mathsf{th}_\mathsf{C}-\Delta) \\ &= 0.5[1 - F_{\tilde{Z}_n}(\mathsf{th}_\mathsf{C}+\Delta) + F_{\tilde{Z}_n}(\mathsf{th}_\mathsf{C}-\Delta)], \end{aligned} \tag{41}$$

which can be calculated using the CDF of the standard form of the noise term.

V. Geometric Power and G-SNR

We first note that all stable distributions, apart from the case $\alpha = 2$, have infinite variance, and all stable distributions with $\alpha \le 1$ also have infinite mean. In fact, this statement can be generalized to moments of order $p \le \alpha$, see [37]. Therefore, the conventional notion of power, which is based on the variance of a signal, is not informative in the case of stable RVs with $\alpha < 2$ as, regardless of the specific distribution, the conventional power is infinity. In this section we use a more generalized definition of power, the *geometric power*, as proposed in [37, Section III]. This definition uses zero-order statistics, i.e., it is based on logarithmic "moments" of the form $\mathbb{E}[\log|N|]$.

Definition 4 (Geometric Power): The geometric power of the RV N is given by:

$$S_0(N) \triangleq e^{\mathbb{E}[\log|N|]}. \tag{42}$$

In the following we use the terms *noise power* and the geometric power of the noise interchangeably.[2]

In [37, Prop. 1], an expression for the geometric power of a symmetric stable distribution is presented. Property 3 implies that symmetric stable distributions are in fact $\mathscr{S}(0, c, \alpha, 0)$. This expression can therefore be used to calculate the geometric power of the noise term L_N in system B. Yet, this expression is not applicable for the noise terms of systems A and C in which $\beta \neq 0$. The following theorem characterizes the geometric power of almost all stable distributions:

Theorem 6: Let $N \sim \mathscr{S}(0, c, \alpha, \beta)$, where $\alpha \neq 1$, or $\alpha = 1$ and $\beta = 0$. Then, the geometric power of N is given by:

$$S_0(N) = cG_\gamma^{(1/\alpha-1)}\big(1 + \beta^2\tan^2(\tfrac{\pi\alpha}{2})\big)^{1/(2\alpha)}, \tag{43}$$

where $G_\gamma = e^\gamma$, and $\gamma \approx 0.5772$ is the Euler's constant [46, Ch. 5.2].

Proof: The proof is provided in Appendix D. ■

Remark 5: For the systems considered in this paper, since $\alpha = \frac{1}{2}$, the noise power simplifies to:

$$S_0(N) = cG_\gamma\big(1 + \beta^2\big). \tag{44}$$

Note that in this case, the noise power increases with respect to β (the degree of skewness) and c (the scale parameter).

We now define the geometric SNR (G-SNR) as in [37, Section III]:

Definition 5 (Geometric Signal-to-Noise Ratio): Let X be the input signal in an additive-noise channel with a random noise N. Then the G-SNR is defined as:

$$\text{G-SNR} \triangleq \frac{1}{2G_\gamma}\left(\frac{X_\max - X_\min}{S_0(N)}\right)^2, \tag{45}$$

where $X_\max$ and $X_\min$ are the maximum and minimum admissible values for the channel input X. The normalizing term $\frac{1}{2G_\gamma}$ is used to ensure that the G-SNR corresponds to the standard SNR in the case of an additive Gaussian noise channel.

Using this definition and Theorem 6, the G-SNR for systems A and C is defined as follows:

$$\text{G-SNR}_A = \frac{1}{2G_\gamma}\left(\frac{\Delta}{2c_\mathrm{A}G_\gamma}\right)^2, \tag{46}$$

$$\text{G-SNR}_C = \frac{1}{2G_\gamma}\left(\frac{2\Delta}{c_\mathrm{C}G_\gamma(1+\beta_\mathrm{C}^2)}\right)^2. \tag{47}$$

[2]Note that the definition of geometric power/SNR we introduce here is different from the one widely used in RF communications.

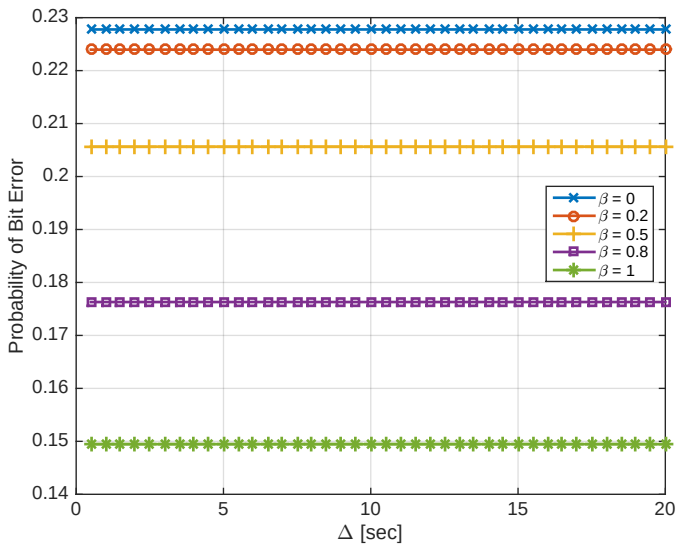

Fig. 5. This plot shows that for a constant G-SNR, the BER is constant. For each point, the parameter c of the noise distribution is calculated using the corresponding value for Δ such that the G-SNR$=1$.

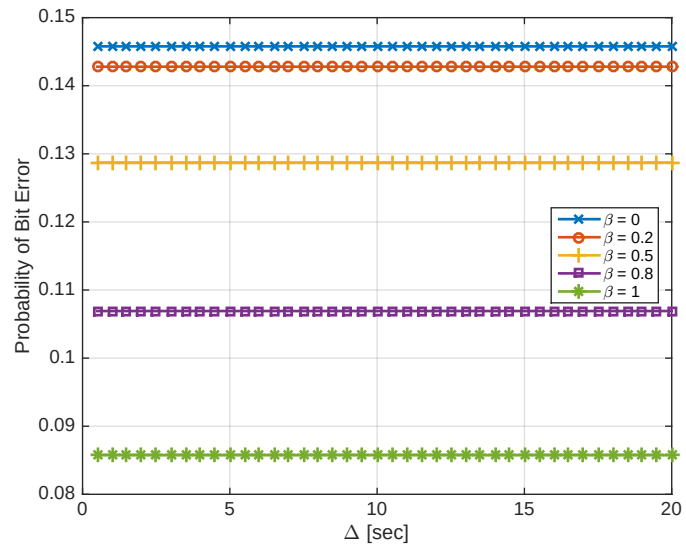

Fig. 6. This plot shows that for a constant G-SNR, the BER is constant. For each point, the parameter c of the noise distribution is calculated using the corresponding value for Δ such that the G-SNR$=10$.

Remark 6: Note that system B involves an absolute value operation, thus, the G-SNR of system B cannot be obtained based on the techniques used to derive the G-SNR for systems A and C. Since the absolute value operation can only degrade the detection performance, calculating the G-SNR of the system $L_y = L_x + L_n$ can serve as an upper bound on the G-SNR of system B. This upper bound is given by:

$$\text{G-SNR}_B \leq \text{G-SNR}_B^{\text{ub}} = \frac{1}{2G_\gamma}\left(\frac{\Delta}{c_{\text{B}}G_\gamma}\right)^2. \tag{48}$$

This implies that the BER of the ML detector for system B is higher than the BER of the ML detector for the system $L_y = L_x + L_n$, as indicated in Section VI.

Remark 7: When the diffusion coefficient and the distance between the transmitter and the receiver are the same, the G-SNR of system A is four times larger than the G-SNR of system B since $c_{\text{B}} = 4c_{\text{A}}$. This implies that on top of the fact that two information particles are released in system B while only a single particle is released in system A, the gain from synchronization is a factor of $\frac{1}{4}$ in the noise geometric power.

Remark 8: For system C let $r = D_a/D_b$ be the ratio of the diffusion coefficient of the two information particles. Then the noise parameters can be written as $c_{\text{C}} = \frac{d^2(\sqrt{r}+1)^2}{2rD_b}$ and $\beta_{\text{C}} = \frac{\sqrt{r}-1}{\sqrt{r}+1}$. Next, assume that the diffusion coefficient D_b is fixed, and the diffusion coefficient of D_a can be changed. In this case the noise geometric power is proportional to $\frac{1}{r}$, which decreases as r increases. This also implies that the G-SNR increases with r. From the expression for β_{C} and c_{C} we observe that $\beta_c \to 1$ and $c_{\text{C}} \to \frac{d^2}{2D_b}$, when $r \to \infty$. Thus, in this case, system C reduces to system A, while no synchronization is required between the transmitter and the receiver. Yet, this comes at a cost of using two different information particles. Note that this cost is captured in the G-SNR expression since the geometric power of the transmitted signal in system C is four times that of systems A and B, which can result in as much as 4 times improvement in G-SNR.

VI. Numerical Evaluation

We start this section by evaluating the affects of the G-SNR, provided in (45), on the BER performance of the three modulation schemes. In the additive white Gaussian noise channel the BER of the ML detector is only a function of SNR, namely, for a fixed SNR, the individual values of the signal power and the noise power do not affect the BER. To evaluate if this property also holds for the three MT systems, we consider system C which can be specialized to both systems A and B using different values of the parameter β_{C}, see (46)–(47). Thus, we evaluate if a constant BER is observed for a fixed value of G-SNR.

Figs. 5 and 6 depict BER versus Δ for two values of G-SNR: 1 and 10. In these plots, the x-axis corresponds to the values of Δ. For each point in the plot, the value of the noise parameter c_{C} is calculated such that G-SNR is either 1 (Figure 5) or 10 (Figure 6). The BER is then numerically calculated using these values based on (41). It can clearly be observed that the BER is constant for a given G-SNR *regardless* of the value of Δ and c_{C}. It can further be observed that the BER decreases as $\beta_{\text{C}} \to 1$, which is in agreement with Remark 8.

Figure 7 depicts the BER versus G-SNR for the different modulation techniques. For system C, five different values of $\beta_{\text{C}} = 0, 0.25, 0.5, 0.75, 0.95$ are considered. The asynchronous scheme in system B with indistinguishable particles achieves the highest BER, while system A, which assumes perfect synchronization, achieves the lowest BER. The gap between these can be thought of as the cost of having no synchronization. Note that in system A, a single particle is released, while in system B two particles are released.

For system C it can be observed that by using two distinguishable particles, the BER improves compared to system B. Note that when $\beta_{\text{C}} = 0$ the noise distribution is the

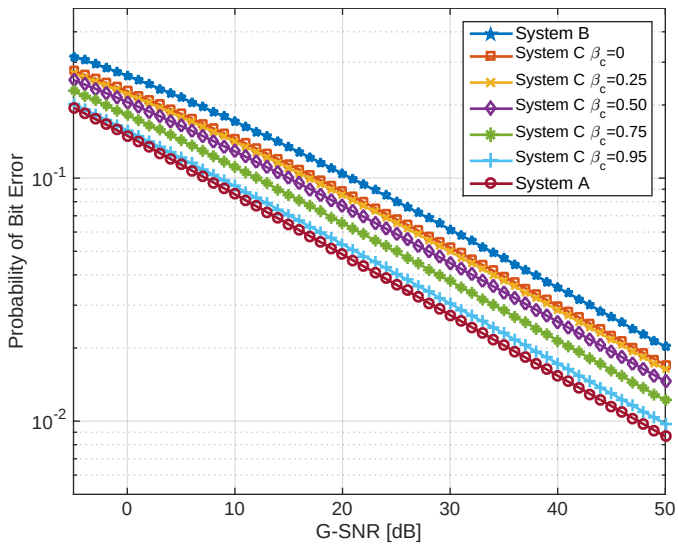

Fig. 7. BER versus G-SNR in dB for each modulation scheme.

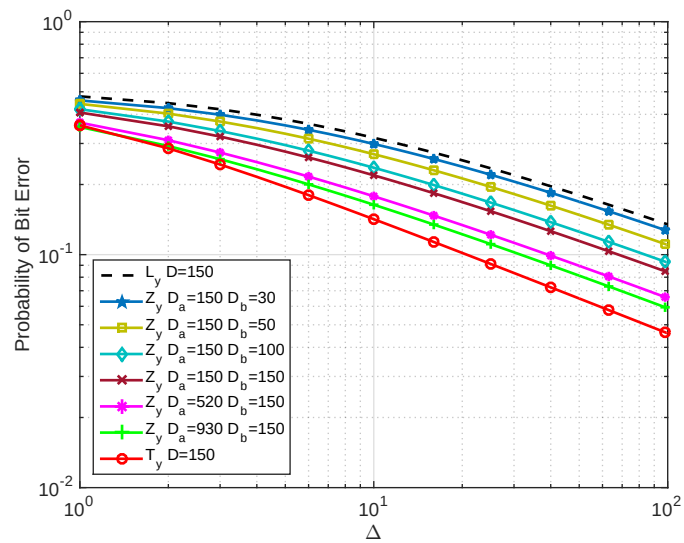

Fig. 8. BER versus Δ under different modulation schemes.

same as that in system B. In this case, when the dispersion parameter c is the same for both systems, the G-SNR of system C is four times larger than $\text{G-SNR}_B^{\text{ub}}$ in (48). Yet, Figure 7 indicates that even for $\beta_{\text{C}} = 0$ the BER of system C is lower than the BER of system B. This demonstrates the destructive effect of the absolute value operation as indicated in Remark 6. Finally, we observe that as β_{C} increases the BER of system C decreases, while when $\beta_{\text{C}} \to 1$ the BER of system C approaches the BER of system A. In this case, asynchronous communication is possible with the same BER performance as synchronized communication at the cost of using two distinguishable particles.

We conclude the numerical evaluations with a case study. We consider a DBMT system where the distance between the transmitter and the receiver is $d = 20$ μm. Assume that the receiver is capable of detecting insulin molecules, which has a diffusion coefficient of $D_I = 150$ μm^2/s [3]. From these values the noise parameters c_{A} and c_{B} can be calculated for the modulation techniques represented by systems A and B. For system C, we consider six different particles as candidates for the second distinguishable particle. These particles are assumed to have diffusion coefficients ranging from 30 μm^2/s (e.g., diffusion coefficient of DNA) to 930 μm^2/s (e.g., diffusion coefficient of glycerol).

Figure 8 depicts the results. Again it can be observed that the asynchronous modulation scheme in system B with indistinguishable particles has the highest BER. Note that even the modulation scheme in system C where the diffusion coefficient of the second particle is one fifth of the diffusion coefficient of the particles used in system B (i.e. 30 μm^2/s) has lower BER. For the modulation technique in system C, as the diffusion coefficient of the second particle increases, the BER decreases. The modulation in system A achieves the best BER performance, and this shows that transmitter-receiver synchronization could have a considerable effect on BER. Table I quantifies the BER for each case.

Δ	1	25	50	75	100
System A	0.3590	0.0912	0.0648	0.0530	0.0460
System B	0.4778	0.2346	0.1799	0.1523	0.1348
System C ($D = 30$)	0.4592	0.2202	0.1687	0.1428	0.1263
System C ($D = 150$)	0.4073	0.1535	0.1145	0.0957	0.0841
System C ($D = 930$)	0.3533	0.1109	0.0812	0.0674	0.0589

TABLE I
THE BER OF DIFFERENT MODULATIONS IN THE CASE STUDY FOR DIFFERENT VALUES OF Δ. FOR THE MODULATION SCHEME IN SYSTEM C THE TERM IN THE PARENTHESIS IS THE DIFFUSION COEFFICIENT OF THE SECOND PARTICLE.

VII. Conclusions and Future Work

In this work, we considered two new asynchronous timing-based modulation techniques based on the time between release of two similar information particles, and the time between release of two different information particles. For evaluation, we compared the performance of these systems to the synchronized modulation based on the time of release of information particles. We showed that the three modulation techniques can be modeled as systems with an additive noise term, where for diffusion-based propagation, the noise terms are stable distributed. For the asynchronous systems, we derived the PDF of the additive noise in terms of the Voigt functions, which can be calculated efficiently and in some special cases be approximated using elementary functions. Using these PDFs we then characterized the ML detectors for each system. Since stable distributions, with the exception of the Gaussian distribution, have infinite variance, we used geometric power as a measure of strength of the noise. Using this approach, we derived the G-SNR for each modulation scheme for comparison. Numerical evaluations show that for a constant G-SNR the BER is constant. Therefore, the G-SNR in DBMT channels plays a similar role as the SNR in the additive Gaussian noise channels. Finally, we showed that, as expected, synchronization has a considerable effect on BER, where the first modulation scheme achieves the lowest BER. Moreover, we showed that it is possible to achieve a similar

BER asynchronously if two distinguishable particles are used per bit.

As part of future work, we will explore extending the results to the case where multiple information particles are released simultaneously instead of one. Note that some of our current ongoing work has shown that simultaneously releasing multiple particles can improve the performance of the first system significantly [24], [45]. We would like to extend these results to the asynchronous systems presented in this paper using order statistics.

Appendix A
Proof of Theorem 2

We use Property 2, and find an expression for the standardized distribution with $c_{\mathrm{B}} = 1$. Then the PDF for any value of c_{B} can be calculated using (8). Let $X \sim \mathscr{S}(0, 1, \frac{1}{2}, 0)$ be a standardized stable RV with parameters $\alpha = \frac{1}{2}$ and $\beta = 0$. Then the PDF of X is given by [47, Eq. (7.1)]:

$$f(x; 1/2, \beta) = \Re\left\{\frac{z}{\pi x}[\sqrt{\pi}e^{-z^2} - 2jD(z)]\right\}, \tag{49}$$

where

$$D(z) = e^{-z^2}\int_0^z e^{t^2}dt \tag{50}$$

is the Dawson's Integral [46, Eq. (7.2.5)], and

$$z = \frac{1+\beta - j(1-\beta)}{2\sqrt{2x}}. \tag{51}$$

It is possible to rewrite (49) in terms of the complex error function, also known as Faddeeva function or the Kramp function [46, Eq. (7.2.3)]:

$$w(z) = e^{-z^2}\left(1 + \frac{2j}{\sqrt{\pi}}\int_0^z e^{t^2}dt\right) = e^{-z^2}\operatorname{erfc}(-jz). \tag{52}$$

Using [46, Eq. (7.5.1)]:

$$D(z) = 0.5j\sqrt{\pi}(e^{-z^2} - w(z)), \tag{53}$$

and the property $w(-z) = 2e^{-z^2} - w(z)$, we rewrite (49) as:

$$f(x; 1/2, \beta) = \Re\left\{\frac{z}{\sqrt{\pi x}}w(-z)\right\}. \tag{54}$$

One of the benefits of writing the PDF in terms of the complex error function is that there are a large body of works that considered calculating it numerically. Moreover, if $z = a + jb$, for $b > 0$ the complex error function can be represented by its real and imaginary parts as [33, Sec. 1]:

$$w(a + jb) = K(a, b) + jL(a, b), \quad b > 0, \tag{55}$$

where $K(a, b)$ and $L(a, b)$ are the real and imaginary Voigt functions given in (14) and (15), respectively.

Using Property 3, the PDF of X is symmetric. Hence, the density for $X \geq 0$ is sufficient for characterizing the whole PDF. Since $\beta = 0$, when $X > 0$, we can write $z = p_x - jp_x$ where $p_x = 1/\sqrt{8x}$. Substituting (55) in (54), the density of X, when $X \geq 0$, can be written as:

$$f(x) = \begin{cases} \frac{1}{\sqrt{8\pi x^3}}\left[K(-p_x, p_x) + L(-p_x, p_x)\right] & x > 0 \\ \frac{2}{\pi} & x = 0 \end{cases}, \tag{56}$$

where the value for $x = 0$ follows from [41, Eq. (2.2.11)]. Finally, the density for $X < 0$ is obtained using symmetry. The proof is completed by applying (8).

Appendix B
Proof of Theorem 4

We use Property 2, and find an expression for the standardized distribution with $c_{\mathrm{C}} = 1$. Thus, the PDF for any value of c_{C} can be calculated using (8). Let $X \sim \mathscr{S}(0, 1, \frac{1}{2}, \beta_{\mathrm{C}})$ be the standardized stable RV with parameters $\alpha = \frac{1}{2}$ and β_{C}. Using (54), and recalling that $\beta_{\mathrm{C}} = (\sqrt{D_a} - \sqrt{D_b})/(\sqrt{D_a} + \sqrt{D_b})$, we write (51) as $z = p_x - jq_x$ when $x > 0$, where $p_x = (1+\beta_{\mathrm{C}})/(\sqrt{8|x|})$ and $q_x = (1-\beta_{\mathrm{C}})/(\sqrt{8|x|})$. Similarly, we write (51) as $z = -q_x - jp_x$ when $x < 0$. Using (54) and the Voigt functions decomposition of the Faddeeva function (55), the PDF of the standardized distribution is given by:

$$f(x; \beta_{\mathrm{C}}) = \begin{cases} \frac{1}{\sqrt{8\pi x^3}}\Big[(1+\beta_{\mathrm{C}})K(-p_x, q_x) \\ \qquad + (1-\beta_{\mathrm{C}})L(-p_x, q_x)\Big], & x > 0 \\ \frac{2(1-\beta^2)}{\pi(1+\beta^2)^2}, & x = 0 \\ \frac{1}{\sqrt{8\pi|x|^3}}\Big[(1-\beta_{\mathrm{C}})K(q_x, p_x) \\ \qquad - (1+\beta_{\mathrm{C}})L(q_x, p_x)\Big], & x < 0 \end{cases},$$

where, again, the value for $x = 0$ follows from [41, Eq. (2.2.11)]. The proof is completed by applying (8).

Appendix C
Proof of Theorem 5

We first observe that for $\ell_y = 0$, $f_{L_y|L_x}(0|0) > f_{L_y|L_x}(0|\Delta)$. This follows from the fact that stable distributions are unimodal, and the mode of the noise term L_n is at $\ell = 0$. Therefore, the threshold is located at $\mathsf{th}_{\mathrm{B}} > 0$, and we focus of the case where $\ell_y > 0$. Note that in this case, due to the continuity and unimodality of stable distributions [41, Theorem 2.7.6], both $f_{L_y|L_x}(\ell_y|L_x = 0)$ and $f_{L_y|L_x}(\ell_y|L_x = \Delta)$ are continuous functions and unimodal. We now have the following lemma:

Lemma 1: If $0 < \ell_y \leq \frac{\Delta}{2}$, then $f_{L_y|L_x}(\ell_y|L_x = 0) > f_{L_y|L_x}(\ell_y|L_x = \Delta)$.

Proof: We first consider the system in (2) without the absolute value: $\tilde{L}_y = L_x + L_n$. Here, $f_{\tilde{L}_y|L_x}(\tilde{l}_y|l_x) = f_{L_n}(\tilde{l}_y - l_x)$. Since stable distributions are unimodal, we have $f_{\tilde{L}_y|L_x}(\tilde{l}_y|L_x = 0) > f_{\tilde{L}_y|L_x}(\tilde{l}_y|L_x = \Delta), \forall \tilde{l}_y < \frac{\Delta}{2}$. Using the expression for the PDF of system (2) in (33)–(34) we obtain the desired result. ■

Lemma 2: If $\ell_y > \frac{\Delta}{2}$, then there exists a point th_{B} such that for all $\frac{\Delta}{2} < \ell_y < \mathsf{th}_{\mathrm{B}}$, $f_{L_y|L_x}(\ell_y|L_x = 0) > f_{L_y|L_x}(\ell_y|L_x = \Delta)$ and for all $\ell_y > \mathsf{th}_{\mathrm{B}}$, $f_{L_y|L_x}(\ell_y|L_x = 0) \leq f_{L_y|L_x}(\ell_y|L_x = \Delta)$.

Proof: Note that for $\ell_y > \frac{\Delta}{2}$, $f_{L_n}(\ell_y) < f_{L_n}(\ell_y - \Delta)$. Moreover, note that $f_{L_n}(\ell)$ is a smooth function and it is decreasing for $\ell > 0$. Then clearly there exists a $\mathsf{th}_{\mathrm{B}} > \frac{\Delta}{2}$ such that:

$$\begin{cases} f_{L_n}(\ell_y) - f_{L_n}(\ell_y - \Delta) > f_{L_n}(\ell_y + \Delta) - f_{L_n}(\ell_y) & \ell_y < \mathsf{th_B} \\ f_{L_n}(\ell_y) - f_{L_n}(\ell_y - \Delta) \leq f_{L_n}(\ell_y + \Delta) - f_{L_n}(\ell_y) & \ell_y \geq \mathsf{th_B}, \end{cases} \tag{57}$$

which follows since the slope of $f_{L_n}(\ell)$ for $\ell > 0$ decreases, reaches a minimum, and then increases. Combining both Lemmas, the theorem is proved. ■

Appendix D
Proof of Theorem 6

To prove this theorem, we first derive $\mathbb{E}[|N|^s]$. We write this expectation in integral form as:

$$\begin{aligned} \mathbb{E}[|N|^s] &= \int_{-\infty}^{\infty} |n|^s f(n; 0, c, \alpha, \beta) dn \\ &\overset{(a)}{=} \int_0^{\infty} n^s f(n; 0, c, \alpha, \beta) dn \\ &\quad + \int_0^{\infty} n^s f(n; 0, c, \alpha, -\beta) dn, \end{aligned}$$

where (a) follows since $f(-x; 0, c, \alpha, \beta) = f(x; 0, c, \alpha, -\beta)$ [26, Proposition 1.11]. Taking the derivative with respect to s we obtain:

$$\begin{aligned} \frac{d}{ds}\mathbb{E}[|N|^s] &= \int_0^{\infty} n^s \log n f(n; 0, c, \alpha, \beta) dn \\ &\quad + \int_0^{\infty} n^s \log n f(n; 0, c, \alpha, -\beta) dn. \end{aligned}$$

Further setting $s = 0$ results in:

$$\frac{d}{ds}\mathbb{E}[|N|^s]\Big|_{s=0} = \mathbb{E}[\log(|N|)].$$

We now define $\lambda \triangleq c^{\alpha}\sqrt{1 + \frac{\beta^2}{\cot^2(\frac{\pi\alpha}{2})}}$, and let

$$\theta \triangleq 2\arctan\left(\frac{\beta}{\cot(\frac{\pi\alpha}{2})}\right)/(\pi\alpha).$$

Using [41, Fact 3, pg. 117], and [41, Theorem 2.6.4] we have that for $N \sim \mathscr{S}(0, c, \alpha, \beta)$, $\alpha \neq 1$,

$$\mathbb{E}[|N|^s] = \lambda^{s/\alpha} \frac{\cos(\frac{\pi}{2}\theta s)\Gamma(1 - s/\alpha)}{\cos(\frac{\pi}{2}s)\Gamma(1 - s)}. \tag{58}$$

By taking the derivative of (58) with respect to s and evaluating the result at $s = 0$ we obtain:

$$\begin{aligned} \mathbb{E}[\log(|N|)] = \log(c) + \frac{1}{2\alpha}\log\left(1 + \frac{\beta^2}{\cot^2(\frac{\pi\alpha}{2})}\right) \\ + (1/\alpha - 1)\gamma, \end{aligned} \tag{59}$$

where γ is the Euler's constant [46, Ch. 5.2]. Finally, recalling that $S_0(N) = e^{\mathbb{E}[\log(|N|)]}$ we conclude the proof.

Acknowledgment

The authors would like to thank Professor John P. Nolan at American University for providing valuable correspondence on stable distributions.

References

[1] N. Farsad, W. Guo, C. B. Chae, and A. Eckford, "Stable distributions as noise models for molecular communication," in *Proc. IEEE Global Communications Conference (GLOBECOM)*, Dec 2015, pp. 1–6.

[2] N. Farsad, Y. Murin, W. Guo, C. B. Chae, A. Eckford, and A. Goldsmith, "On the impact of time-synchronization in molecular timing channels," in *Proc. IEEE Global Communications Conference (GLOBECOM)*, 2016, pp. 1–6.

[3] N. Farsad, H. B. Yilmaz, A. Eckford, C.-B. Chae, and W. Guo, "A comprehensive survey of recent advancements in molecular communication," *IEEE Communications Surveys & Tutorials*, vol. 18, no. 3, pp. 1887–1919, 3Q 2016.

[4] T. Nakano, A. Eckford, and T. Haraguchi, *Molecular communication*. Cambridge University Press, 2013.

[5] W. Guo, T. Asyhari, N. Farsad, H. B. Yilmaz, A. Eckford, and C.-B. Chae, "Molecular communications: Channel model and physical layer techniques," *IEEE Wireless Communications*, vol. 23, no. 4, pp. 120–127, Aug. 2016.

[6] M. S. Kuran, H. B. Yilmaz, T. Tugcu, and I. F. Akyildiz, "Interference effects on modulation techniques in diffusion based nanonetworks," *Nano Communication Networks*, vol. 3, no. 1, pp. 65–73, Mar. 2012.

[7] N.-R. Kim and C.-B. Chae, "Novel modulation techniques using isomers as messenger molecules for nano communication networks via diffusion," *IEEE Journal on Selected Areas in Communications*, vol. 31, no. 12, pp. 847–856, Dec. 2013.

[8] N. Farsad, A. Eckford, S. Hiyama, and Y. Moritani, "On-chip molecular communication: Analysis and design," *IEEE Transactions on NanoBioscience*, vol. 11, no. 3, pp. 304–314, Feb. 2012.

[9] A. W. Eckford, "Timing information rates for active transport molecular communication," in *Nano-Net*, ser. Lecture Notes of the Institute for Computer Sciences, Social Informatics and Telecommunications Engineering. Springer Berlin Heidelberg, 2009, vol. 20, pp. 24–28.

[10] M. U. Mahfuz, D. Makrakis, and H. T. Mouftah, "On the characterization of binary concentration-encoded molecular communication in nanonetworks," *Nano Communication Networks*, vol. 1, no. 4, pp. 289–300, Dec. 2010.

[11] N. Farsad, A. W. Eckford, and S. Hiyama, "Channel design and optimization of active transport molecular communication," in *Proc. of 6th International ICST Conference on Bio-Inspired Models of Network, Information, and Computing Systems*, York, England, 2011.

[12] P. Lio and S. Balasubramaniam, "Opportunistic routing through conjugation in bacteria communication nanonetwork," *Nano Communication Networks*, vol. 3, no. 1, pp. 36–45, 2012. [Online]. Available: http://www.sciencedirect.com/science/article/pii/S1878778911000561

[13] A. Bicen and I. Akyildiz, "System-theoretic analysis and least-squares design of microfluidic channels for flow-induced molecular communication," *IEEE Transactions on Signal Processing*, vol. 61, no. 20, pp. 5000–5013, Oct 2013.

[14] N. Farsad, W. Guo, and A. W. Eckford, "Tabletop molecular communication: Text messages through chemical signals," *PLOS ONE*, vol. 8, no. 12, p. e82935, Dec 2013.

[15] N. Farsad, W. Guo, and A. Eckford, "Molecular communication link," in *Proc. IEEE Conference on Computer Communications (INFOCOM)*, 2014, pp. 107–108, live demo.

[16] B. H. Koo, C. Lee, H. B. Yilmaz, N. Farsad, A. Eckford, and C.-B. Chae, "Molecular MIMO: From theory to prototype," *IEEE Journal on Selected Areas in Communications*, vol. 34, no. 3, pp. 600–614, March 2016.

[17] B. Atakan, S. Galmes, and O. Akan, "Nanoscale communication with molecular arrays in nanonetworks," *IEEE Transactions on NanoBioscience*, vol. 11, no. 2, pp. 149–160, June 2012.

[18] B. Krishnaswamy, C. Austin, J. Bardill, D. Russakow, G. Holst, B. Hammer, C. Forest, and R. Sivakumar, "Time-elapse communication: Bacterial communication on a microfluidic chip," *IEEE Transactions on Communications*, vol. 61, no. 12, pp. 5139–5151, Dec. 2013.

[19] K. V. Srinivas, A. Eckford, and R. Adve, "Molecular communication in fluid media: The additive inverse Gaussian noise channel," *IEEE Transactions on Information Theory*, vol. 58, no. 7, pp. 4678–4692, July 2012.

[20] H. Li, S. Moser, and D. Guo, "Capacity of the memoryless additive inverse Gaussian noise channel," *IEEE Journal on Selected Areas in Communications*, vol. 32, no. 12, pp. 2315–2329, Dec 2014.

[21] N. Farsad, Y. Murin, A. Eckford, and A. Goldsmith, "On the capacity of diffusion-based molecular timing channels," *IEEE International Symposium on Information Theory Proceedings (ISIT)*, 2016.

[22] C. Rose and I. S. Mian, "Inscribed Matter Communication: Part I," *IEEE Transactions on Molecular, Biological and Multi-Scale Communications*, vol. 2, no. 2, pp. 209–227, Dec. 2016.

[23] ——, "Inscribed Matter Communication: Part II," *IEEE Transactions on Molecular, Biological and Multi-Scale Communications*, vol. 2, no. 2, pp. 228–239, Dec. 2016.

[24] N. Farsad, Y. Murin, A. Eckford, and A. Goldsmith, "Capacity limits of diffusion-based molecular timing channels," *IEEE Transactions on Information Theory*, submitted. [Online]. Available: http://arxiv.org/abs/1602.07757

[25] Y. Murin, N. Farsad, M. Chowdhury, and A. Goldsmith, "Time-slotted transmission over molecular timing channels," *Nano Communication Networks*, vol. 12, pp. 12–24, June 2017.

[26] J. P. Nolan, *Stable Distributions - Models for Heavy Tailed Data*. Boston: Birkhauser, 2015, in progress, Chapter 1 online at academic2.american.edu/∼jpnolan.

[27] H. He, J. Lu, J. Chen, X. Qiu, and J. Benesty, "Robust blind identification of room acoustic channels in symmetric alpha-stable distributed noise environments," *The Journal of the Acoustical Society of America*, vol. 136, no. 2, pp. 693–704, 2014. [Online]. Available: http://scitation.aip.org/content/asa/journal/jasa/136/2/10.1121/1.4884760

[28] S. Niranjayan and N. Beaulieu, "The BER optimal linear rake receiver for signal detection in symmetric alpha-stable noise," *IEEE Transactions on Communications*, vol. 57, no. 12, pp. 3585–3588, Dec. 2009.

[29] L. Fan, X. Li, X. Lei, W. Li, and F. Gao, "On distribution of SaS noise and its application in performance analysis for linear rake receivers," *IEEE Communications Letters*, vol. 16, no. 2, pp. 186–189, Feb. 2012.

[30] J. Wang, E. Kuruoglu, and T. Zhou, "Alpha-stable channel capacity," *IEEE Communications Letters*, vol. 15, no. 10, pp. 1107–1109, Oct. 2011.

[31] J. Fahs and I. Abou-Faycal, "On the capacity of additive white alpha-stable noise channels," in *Proc. IEEE International Symposium on Information Theory Proceedings (ISIT)*, July 2012, pp. 294–298.

[32] F. Schrier, "The voigt and complex error function: A comparison of computational methods," *Journal of Quantitative Spectroscopy and Radiative Transfer*, vol. 48, no. 5/6, pp. 743–762, Nov.-Dec. 1992.

[33] S. Abrarov and B. Quine, "Efficient algorithmic implementation of the voigt/complex error function based on exponential series approximation," *Applied Mathematics and Computation*, vol. 218, no. 5, pp. 1894–1902, 2011.

[34] M. R. Zaghloul and A. N. Ali, "Algorithm 916: Computing the faddeyeva and voigt functions," *ACM Trans. Math. Softw.*, vol. 38, no. 2, pp. 15:1–15:22, Jan. 2012. [Online]. Available: http://doi.acm.org/10.1145/2049673.2049679

[35] S. M. Abrarov and B. M. Quine, "A Rational Approximation for Efficient Computation of the Voigt Function in Quantitative Spectroscopy," *Journal of Mathematics Research*, vol. 7, no. 2, pp. 163–174, 2015. [Online]. Available: http://www.ccsenet.org/journal/index.php/jmr/article/view/46896

[36] "An assessment of some closed-form expressions for the voigt function," *Journal of Quantitative Spectroscopy and Radiative Transfer*, vol. 176, pp. 1–5, 2016.

[37] J. Gonzalez, J. Paredes, and G. Arce, "Zero-order statistics: A mathematical framework for the processing and characterization of very impulsive signals," *IEEE Transactions on Signal Processing*, vol. 54, no. 10, pp. 3839–3851, Oct. 2006.

[38] A. Noel, K. Cheung, and R. Schober, "Improving receiver performance of diffusive molecular communication with enzymes," *IEEE Transactions on NanoBioscience*, vol. 13, no. 1, pp. 31–43, March 2014.

[39] I. Karatzas and S. E. Shreve, *Brownian Motion and Stochastic Calculus*. New York: Springer-Verlag, 1991.

[40] H. B. Yilmaz, A. C. Heren, T. Tugcu, and C.-B. Chae, "Three-dimensional channel characteristics for molecular communications with an absorbing receiver," *IEEE Communications Letters*, vol. 18, no. 6, pp. 929–932, June 2014.

[41] V. Zolotarev, *One-dimensional stable distributions*. American Mathematical Soc., 1986, vol. 65.

[42] B. Armstrong, "Spectrum line profiles: The voigt unction," *Journal of Quantitative Spectroscopy and Radiative Transfer*, vol. 7, no. 1, pp. 61–88, 1967.

[43] J. P. Nolan, "Numerical calculation of stable densities and distribution functions," *Communications in statistics. Stochastic models*, vol. 13, no. 4, pp. 759–774, 1997.

[44] Y. Murin, N. Farsad, M. Chowdhury, and A. Goldsmith, "Communication over diffusion-based molecular timing channels," in *Proc. IEEE Global Communications Conference (GLOBECOM)*, 2016, pp. 1–6.

[45] ——, "Communication over molecular timing channels with α-stable noise," 2017, in preparation. [Online]. Available: http://web.stanford.edu/∼moriny

[46] F. W. J. Olver, D. W. Lozier, R. F. Boisvert, and C. W. Clark, Eds., *NIST Handbook of Mathematical Functions*, 1st ed. Cambridge University Press, 2010.

[47] D. R. Holt and E. L. Crow, "Tables and graphs of the stable probability density functions," *Journal of Research of the National Bureau of Standards B*, vol. 77, pp. 143–198, 1973.